water

MDPI

Article

Response Surface Optimization and Floc Structure Analysis of Magnetic Flocculation Technology for Anaerobic Digestion Reject Water

Bo Xu [1,2], Yongzhi Chi [1], Yiyang Chi [3], Jianhai Zhao [1], Cuilian Fu [1], Xueke Wang [4], Sufeng Tian [1] and Yanmei Ding [1,*]

1 Tianjin Key Laboratory of Water Quality Science and Technology, School of Environmental and Municipal Engineering, Tianjin Chengjian University, Tianjin 300384, China
2 Heishan Meteorological Bureau, Liaoning 121400, China
3 International School of Engineering, Tianjin Chengjian University, Tianjin 300384, China
4 Tianjin Enew Environmental Protection Engineering Co., Ltd., Tianjin 300403, China
* Correspondence: yanmeidingtt@126.com

Abstract: In order to improve the removal efficiencies of SS and Fe^{3+} in anaerobic digestion reject water for the subsequent biological treatment process, on the basis of the single factor test in the early stage, the response surface method was used, and the structure of the formed floc was analyzed by magnetic flocculation. The optimum amounts of magnetic powder, polyaluminum chloride (PAC) and polyacrylamide (PAM) were 40.51 mg/L, 31.31 mg/L and 4.05 mg/L, respectively. At this time, the removal efficiencies of SS and Fe^{3+} were 97.84% and 98.35%. The effects of floc particle size, scanning electron microscopy, infrared spectroscopy and two-dimensional fractal dimension of flocs on the flocculation ability showed that: compared with conventional coagulation, the average particle size of flocs treated by magnetic flocculation was 76.56 μm, the Fe-O-Al absorption peak appeared at 984 cm^{-1}, the flocculation ability was significantly improved, the surface of the floc was rough and porous, and the structure was dense, and the sedimentation performance was significantly improved also.

Keywords: magnetic flocculation technology; anaerobic digestion reject water; response surface optimization; floc

check for updates

Citation: Xu, B.; Chi, Y.; Chi, Y.; Zhao, J.; Fu, C.; Wang, X.; Tian, S.; Ding, Y. Response Surface Optimization and Floc Structure Analysis of Magnetic Flocculation Technology for Anaerobic Digestion Reject Water. *Water* **2023**, *15*, 707. https://doi.org/10.3390/w15040707

Academic Editors: Meifang Hou and Xiyan Ji

Received: 30 December 2022
Revised: 6 February 2023
Accepted: 8 February 2023
Published: 10 February 2023

1. Introduction

As a sludge treatment method, anaerobic digestion technology can convert a large amount of organic matter in sludge into biogas, and realize the reduction and resource utilization of sludge [1–3]. The sludge after anaerobic digestion usually has the characteristics of a low carbon-nitrogen ratio, high ammonia-nitrogen concentration and complex composition, and is often treated by autotrophic biological denitrification [4,5]. In order to improve the dewatering performance of anaerobic digestion sludge, ferric chloride is usually added. Although it can effectively improve the sludge dewatering performance, it also results in a large amount of total iron, suspended solids (SS) and colloidal substances remaining in the dewatering liquid [6,7]. It was reported that Fe^{3+} entered the cell along with cell action and directly affected the activity of biological enzymes [8]. Excessive Fe^{3+} was toxic and could produce oxygen-free radicals in the cells, which damaged microbial cells, and led to a decrease in the removal efficiencies of COD and TN [9]. When the Fe^{3+} concentration increased to 40 mg/L, the removal efficiencies of COD and TN decreased to 88% and 81%, respectively [10]. A high SS concentration in wastewater reduces the efficiency of the biological treatment process [11]. The highest impact on the autotrophic biological denitrification process performance among the given possibilities falls on the influent SS concentration. Seventy percent of the plants reported high impact or operational

problems with high influent SS concentrations. Too high influent SS loads showed reduced active biomass in the reactor and then required an extra excess sludge withdrawal [12]. Therefore, it is a necessity to develop a cost-effective pretreatment process to remove the Fe^{3+} and SS and improve the performance of subsequent biological treatment processes in anaerobic digestion reject water treatment.

Traditional approaches for removing Fe^{3+} from wastewater include adsorption [13], membrane filtration [14] and electrochemical treatment [15]. They have been extensively applied to remove Fe^{3+} from Fe^{3+}-contained wastewater, but satisfactory results cannot be obtained since the increasing efficiency, low-cost and quality index requirements of reject water treatment. Gravity sedimentation was widely applied in the removal of SS in wastewater. However, the gravity sedimentation of SS is generally a time-consuming process [16]. Sand filtration and low-pressure membrane filtration facilitate more efficient solid-liquid separation than gravity sedimentation [17]. Nonetheless, the introduction of these processes in reject water treatment is limited because of the high operation cost derived from inevitable filter clogging or membrane fouling. The conventional coagulation process can effectively reduce the pollutant content in the dewatering liquid, but the problems of long settling time, large floor space, high cost of coagulant and difficult recovery still exist [18–20]. Magnetic flocculation technology is to add magnetic powder on the basis of conventional coagulation, uses the magnetic properties and specific surface area of the magnetic powder itself, improves the Lorentz force, increases the chance of collision between particles, and condenses small pollutants into larger flocs. By self-precipitating or adding a magnetic field, the effect of sedimentation, separation and removal of pollutants can be improved [21–23]. Magnetic flocculation has the advantages of simple operation, small footprint, stable effluent effect and fast floc settling speed. After the introduction of magnetic powder, it can be reused after proper treatment [24–26]. It can be used in surface water clarification, sewage treatment and stormwater. It is widely used in precipitation and other aspects [27,28].

The treatment effect of the magnetic flocculation process is affected by many factors, including the type and dosage of the flocculant [29,30]. In this paper, three coagulation methods (PAC, PAC + PAM, and magnetic flocculation (magnetic powder + PAC + PAM)) were used to treat the dewatering liquid of anaerobic digestion sludge, and the optimization of the dosage of chemicals was carried out by the response surface method. The structure of the formed flocs was analyzed, the composition and properties of the flocs under different coagulation methods were studied, and the reaction mechanism of magnetic flocculation was explored. The aim was to reduce the dosage of chemicals on the basis of ensuring the removal effect, to improve the magnetic flocculation. At the same time, the results could provide reference data and theoretical guidance for practical application [31,32].

2. Materials and Methods

2.1. Laboratory Water Quality

The raw water in the test was taken from the anaerobic digestion sludge dewatering liquid (hereinafter referred to as anaerobic digestion reject water) of a sewage treatment plant in Tianjin (39°12′15″ N, 117°12′20″ E). The anaerobic digestion sludge dewatering unit adopts a plate-and-frame pressure filter. The raw water was taken weekly and stored at room temperature. The raw water appeared to be light yellow. Considering the process characteristics of the subsequent biological treatment unit and the requirements of water intake, the sludge dewatering liquid was pretreated with an aeration capacity of 0.6 L/min (30 min). In this process, Fe^{2+} was oxidized to Fe^{3+} existed, and Fe^{3+} will exist in the form of iron hydroxide after combining with water. The water after aeration was used as the test water. The characteristics of raw water and test water are shown in Table 1.

Table 1. Characteristics of anaerobic digestion reject water.

Indicators	pH	SS (mg/L)	COD (mg/L)	Total Iron (mg/L)	Fe^{2+} (mg/L)
Raw water	7.0 ± 0.2	450 ± 80	387 ± 125	364 ± 32	129 ± 34
Test water	7.0 ± 0.2	450 ± 80	343 ± 62	364 ± 32	<1

2.2. Agents and Instruments

Reagents: polyaluminum chloride (PAC, content not less than 28% aluminum chloride), polyacrylamide (PAM, anionic, average molecular weight 3 million to 12 million), magnetic powder (The purity of Fe_3O_4 was greater than 98%).

Test instruments: Laser particle size analyzer (Mastersizer 2000, Malvern, UK), Scanning electron microscopy (SEM, S-4700), Fourier transform infrared spectroscopy (Nicolet iS 10 FT-IR spectrometer, Thermo Scientific, Waltham, MA, USA), Computer type transreflector polarizing microscope (XPV-600E).

2.3. Methods

2.3.1. Response Surface Optimization

In this test, according to the preliminary orthogonal test results of the research group, the optimal hydraulic conditions of coagulation were determined as follows [33]: fast agitation (300 r/min) for 2 min, slow agitation (100 r/min) for 15 min, and standing for 10 min. According to the single factor test results, the dosage of magnetic powder 30–50 mg/L, PAC 20–40 mg/L and PAM 3–5 mg/L are the optimal range values of three reagents for the treatment of anaerobic digestion reject water by magnetic flocculation technology. On this basis, in this study, magnetic powder dosage (A), PAC dosage (B) and PAM dosage (C) were used as influence factors, SS and Fe^{3+} contents in anaerobic digestion reject water were used as response values X and Y, respectively, and box-Behnken test Design was performed by design-Expert 8.0 [34,35]. Thus, 17 groups of experimental schemes were obtained. The test factors and levels are shown in Table 2. The test scheme and results are shown in Table 3.

Table 2. The test factors and levels.

Level	A /mg·L^{-1}	B /mg·L^{-1}	C /mg·L^{-1}
−1	30	20	3
0	40	30	4
1	50	40	5

2.3.2. Analysis of Floc

In this test, the optimal hydraulic conditions of coagulation were the same as described in Section 2.3.1. According to the response surface optimization results, the optimal dosage of magnetic powder, PAC and PAM can be determined when the removal rate of SS and Fe^{3+} is the highest. According to the optimal dosage of three kinds of reagents, three kinds of floc treated by (A) PAC, (B) PAC + PAM and (C) magnetic powder + PAC + PAM were collected, respectively. The particle size distribution, surface morphology, functional groups, two-dimensional fractal dimension (D_{2f}) and flocculation ability (FA) of the three kinds of flocs were studied.

Particle Size

One liter of the test water was poured into a beaker, followed by the addition of PAC, PAC + PAM and magnetic flocculation, respectively, to ensure the same dosage of each agent, carry out coagulation under optimal hydraulic conditions, take an appropriate amount of the three mixed liquids after stirring and use laser particle size analyzer to

determine the particle size distribution of the respective floc. The particle size distribution of flocs was plotted and analyzed [36].

Table 3. The test scheme and results.

Number	A	B	C	SS /mg·L^{-1}	Fe^{3+} /mg·L^{-1}
1	0	1	−1	26.11	24.68
2	−1	1	0	19.94	18.07
3	0	1	1	21.05	19.85
4	0	−1	−1	26.31	24.96
5	1	0	−1	24.54	22.59
6	0	0	0	10. 46	5.87
7	1	0	1	20.08	18.46
8	−1	0	−1	22.85	19.77
9	1	1	0	15.34	16.54
10	0	0	0	10.39	6. 39
11	1	−1	0	23.16	21.05
12	−1	−1	0	20.38	18.43
13	0	−1	1	27.86	26.85
14	0	0	0	10.32	5.1
15	−1	0	1	23.37	20.94
16	0	0	0	10. 15	6.12
17	0	0	0	9.92	6.18

SEM

SEM was used to observe the surface morphology of flocs by the interaction between electrons and matter. Three kinds of flocculated flocs were extracted and filtered by 0.45 μm microfiltration membrane with suction filter machine. The intercepted flocs were placed in 60 °C electric thermostatic drying oven to dry. Appropriate samples were taken and gold sprayed on the surface (10 s), and then the morphology was scanned, and representative images were selected for analysis.

FTIR

FTIR was employed to analyze functional groups. Three kinds of floc samples were extracted after slow stirring and before settling. Dehumidification was placed in vacuum freeze dryer, and 0.1 g dried potassium bromide (120 °C) was mixed with the sample to be tested, ground and pressed. Three kinds of floc samples (potassium bromide tablets) prepared by Nicolet iS10 FTIR were scanned and analyzed in the wave number range of 500 cm^{-1}~4000 cm^{-1} [37]. Infrared spectra were drawn to analyze the composition of three kinds of floc.

Influence of D_{2f} of Flocs on FA

The fractal dimension was used to reflect the morphology of flocs. Generally speaking, the higher the value of D_{2f} is, the tighter the morphology of flocs is, and the better the sedimentation performance is [38–40]. Jin [41] combined fractal dimension with sludge volume index (SVI) and verified the important role of fractal dimension in flocs settlement.

(1) The determination of D_{2f}

The three kinds of flocs treated by PAC, PAC + PAM and magnetic flocculation were diluted and dispersed on the slides. The images were taken by computer type transreflection-polarizing microscope and processed by image-Pro-Plus software. The functional relationship between the area (A) and perimeter (P) of the floc was investigated, so as to calculate the D_{2f} value of the floc [42,43].

Fractal structure is one of the characteristics of flocs, and flocs with different structures have different fractal dimensions [44,45]. According to the fractal theory, the relation between the area A and the perimeter P of the flocs with fractal structure is:

$$A \propto R^{D2f} \quad (1)$$

In the formula, D_{2f} is two-dimensional fractal dimension. R is the characteristic length, and the numerical value is the perimeter P [46]. Three kinds of flocs treated by (a) PAC, (b) PAC + PAM and (c) magnetic flocculation were diluted, and images were taken by computer permeable polarizing microscope. Then, enough samples with obvious structural characteristics were selected to fit their area A and perimeter P, and then the value of D_{2f} was obtained [43].

(2) The determination of FA

Eighty milliliters of water samples treated by the three methods were taken for ultrasonic treatment at 50 W power for 15 s. Ten milliliters were taken out of each of the three water samples and centrifuged at 1200 r/min for 2 min. Sufficient supernatant was taken out and its absorbance was measured at 650 nm (A). The remaining suspension was stirred at 60 r/min and 15 min, 10 mL of which was centrifuged at 1200 r/min and 2 min. The absorbance of supernatant was measured at 650 nm (B), and the value of FA was calculated by the formula FA = (A − B)/A [47].

3. Results and Discussion

3.1. Analysis of SS and Fe^{3+} Contents in Sludge Dewatering Liquid

3.1.1. Model Variance Analysis of SS

The quadratic multinomial regression equation of SS (X) for the independent variable A (magnetic particle dosage), B (PAC dosage) and C (PAM dosage) is X = +213.27

$$-1.72A - 2.41B - 63.35C - 1.84 \times 10^{-2}AB - 0.12AC - 0.16BC + 3.41 \times 10^{-2}A^2 + 6.03 \times 10^{-2}B^2 + 9.04C^2 \quad (2)$$

It can be seen from Equation (1) that the parabolic opening of the equation is upward, and there is a minimum value. At this point, SS content in sludge dewatering liquid is the lowest, which is the optimal point of the SS removal effect in this test. The variance analysis of the SS regression model is shown in Table 4.

Table 4. Variance analysis of SS regression model.

Source	Sum of Squares	df	Mean Square	*F*	*p*	R^2
Model	668.69	9	74.3	1262.49	<0.0001	0.9994
A	1.46	1	1.46	24.84	0.0016	
B	29.15	1	29.15	495.26	<0.0001	
C	6.94	1	6.94	117.89	<0.0001	
AB	13.62	1	13.62	231.37	<0.0001	
AC	6.2	1	6.2	105.35	<0.0001	
BC	10.92	1	10.92	185.61	<0.0001	
A^2	49.17	1	49.17	835.48	<0.0001	
B^2	153.59	1	153.59	2609.89	<0.0001	
C^2	344.45	1	344.45	5852.99	<0.0001	
Residual	0.41	7	0.059			
Lack of Fit	0.22	3	0.075	1.6	0.3232	
Pure Error	0.19	4	0.047			
Total	669.1	16				

As can be seen from Table 4, the *F* value in the regression model of the response surface is 1262.49 > 0.05, and the significance level is $p < 0.0001$, indicating that the model is significant and can intuitively indicate the accuracy of the test. The *p*-value of the missing

term was 0.3232 > 0.05, indicating that the missing term is not significant, indicating that the quadratic polynomial model obtained by the test has a good fitting degree, which can be used to predict and analyze the removal effect of SS in anaerobic digestion sludge dewatering liquid. The model calibration coefficient R^2_{adj} was 0.9986, indicating that the model can roughly explain 99.86% of the response value changes, and about 0.14% of the response value changes can not be well explained. The correlation coefficient R^2 of the model was 0.9994, indicating that the model has a good fitting effect and is suitable for adoption. The *p* values of AB, BC and AC are all lower than 0.05, indicating that the interaction among magnetic particles, PAC and PAM play a significant role in the SS removal process [48].

The comparison between the experimental value and the predicted value of SS content in the magnetic flocculation process was shown in Figure 1. It can be seen from the image that the slope of the straight line is close to 1, indicating that the model can replace the real value, so as to analyze the three-factor test results.

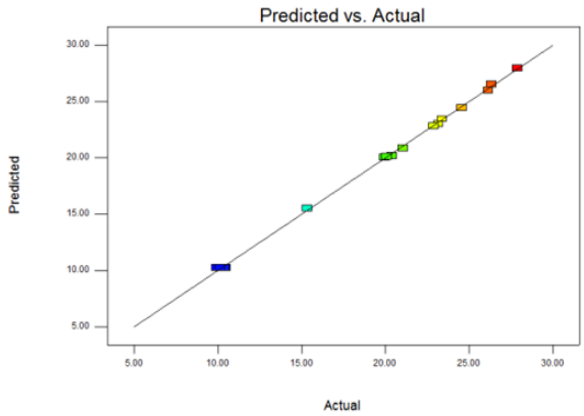

Figure 1. Experimental response values versus predicted response value of SS content.

3.1.2. Response Surface Diagram and Parameter Optimization of SS

The magnetic powder dosage, PAC dosage and PAM dosage were selected as the factors. According to the single factor test results in the early stage, the SS and Fe^{3+} content in reject water was taken as the index to represent the treatment effect of reject water. The response surface diagram was made by Design-Expert 8.0 software. The minimum SS content was taken as the optimization objective in the test, and the response surface map was drawn according to the above model, as shown in Figure 2.

It can be seen from Figure 2 that the extreme value of SS content 3was within the selection range of experimental factors. When the PAM dosing quantity was 4 mg/L, the effect of magnetic powder and liquid PAC dosing quantity on the SS content of reject water was shown in Figure 2a. From Figure 2a, when the PAC dosage remained the same, at first the SS levels decreased with the increase of the magnetic powder levels, after the SS levels reach the minimum value, the SS levels increased with the increase of the magnetic powder levels. The reason is likely that at first when the PAM dosage and PAC dosage were constant, the magnetic particle's ability to absorb negatively charged pollution particles increased with the magnetic powder dosage increase. After the magnetic particle's adsorption capacity reached the maximum value, the excessive addition of magnetic powder can no longer absorb more pollutants. If the addition of magnetic powder continued to increase, the SS content would not be reduced, but the stability of the formed floc would be reduced, the sedimentation process of the floc would be affected, and the flocculation effect would be reduced [49–51]. Similarly, SS content decreased with the increase of PAC content within a certain range and increased when PAC content exceeds a certain range. Figure 2b shows the influence of magnetic powder dosage and PAM dosage on SS in reject water when PAC dosage is 30 mg/L. It can be seen that with the increase of magnetic powder dosage and PAM dosage, SS levels in reject water generally decreased at first and then increased,

and SS levels had an optimal action value. Figure 2c shows the influence of PAC dosage and PAM dosage on SS in reject water when magnetic powder dosage was 40 mg/L. At first, the removal effect of SS increased with the increase of PAC dosage, but when PAC dosage continued to increase, the removal effect of SS decreased. The reason may be the excessive dosage of coagulant PAC affected the electric neutralization effect and changed the charge of the colloidal system. As a result, the removal efficiency of SS in reject water decreased [52,53].

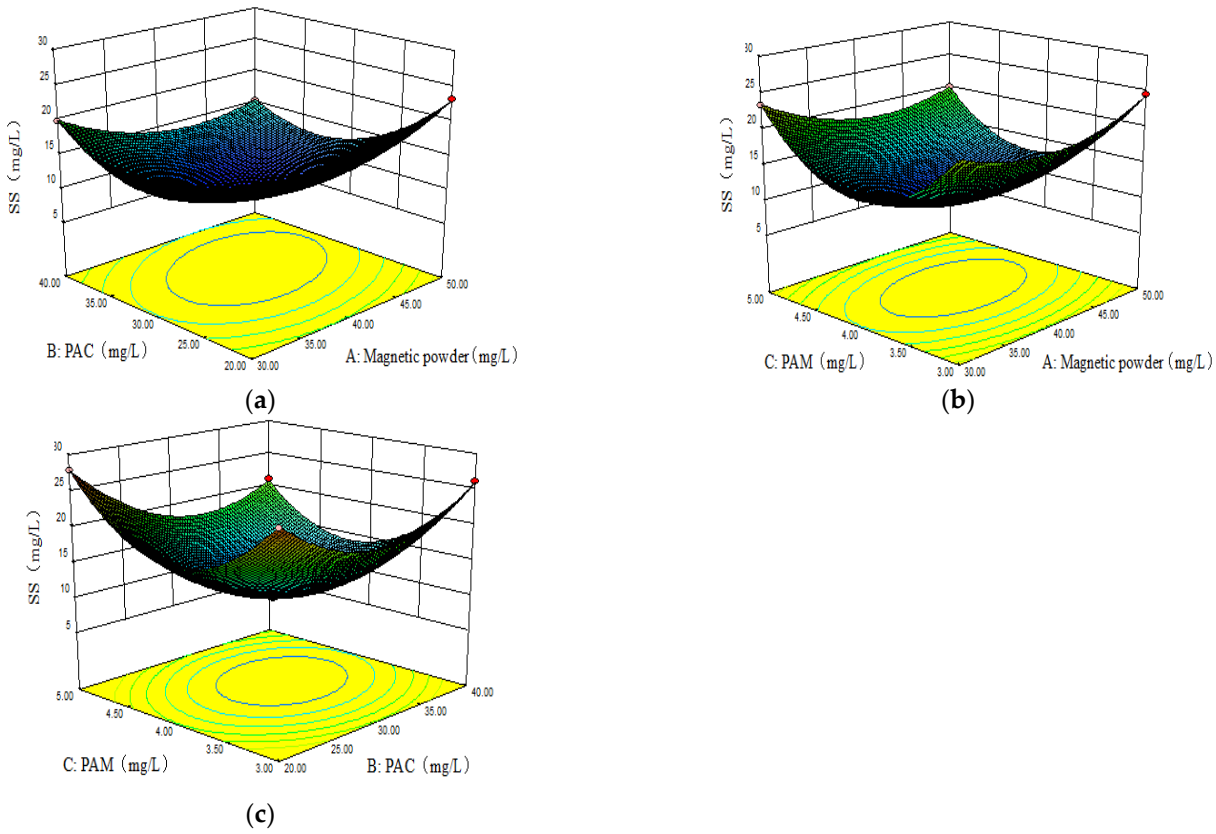

Figure 2. Response surface diagram of interaction among various factors (SS) (**a**) magnetic po3wder and PAC (**b**) magnetic powder and PAM (**c**) PAC and PAM.

According to the response surface diagram of SS content in reject water, the influence of the three factors on SS removal is as follows: PAM > magnetic powder > PAC, which is consistent with the results of model variance analysis in Table 4 [54].

3.1.3. Model Variance Analysis of Fe^{3+}

The quadratic multiple regression equation of Fe^{3+} (Y) to the independent variables A (magnetic powder), B (PAC), C (PAM) is

$$Y = 260.94 - 2.65A - 3.88B - 70.03C - 1.03 \times 10^{-2}AB - 0.13AC - 0.16BC + 4.39 \times 10^{-2}A^2 + 8.03 \times 10^{-2}B^2 + 9.95C^2 \quad (3)$$

In Equation (2), the coefficient of the equation is known, the parabolic opening of the equation is upward, and there is a minimum value, which is the best advantage of this model. The variance analysis of Fe^{3+} is shown in Table 5.

It can be seen from Table 5, the F value of this model is 713.49 > 0.05, and the significance level is $p < 0.0001$, indicating that this model is significant. The p-value of the missing term is 0.0595 > 0.05, indicating that the missing term is not significant, indicating that the quadratic polynomial model obtained by the test has a good fitting degree, which can be used to predict and analyze the removal effect of Fe^{3+} in anaerobic digestion reject water. R^2_{adj} is the calibration determination coefficient of the model, and the value is

0.9975, indicating that the model can roughly explain 99.75% of the response value changes, and about 0.25% of the response value changes cannot be well explained. The correlation coefficient R^2 of this model is 0.9989, indicating that the model has a good fitting effect and high credibility. The *p* value of A in the table is larger than 0.05, indicating that the removal effect of magnetic powder on Fe^{3+} is not significant. The *p* values of B, C, AB, AC and BC were all lower than 0.05, indicating that PAC, PAM and the interaction between magnetic powder and PAC, magnetic powder and PAM, and PAC and PAM played a significant role in the removal process of Fe^{3+}. At this time, the comparison between the experimental value and the predicted value of Fe^{3+} content in the anaerobic digestion reject water was shown in Figure 3.

Table 5. Variance analysis of Fe^{3+} regression model.

Source	Sum of Squares	df	Mean Square	*F*	*p*	R^2
Model	895.41	9	99.49	713.49	<0.0001	0.9989
A	0.26	1	0.26	1.83	0.2178	
B	18.45	1	18.45	132.33	<0.0001	
C	4.35	1	4.35	31.2	0.0008	
AB	4.31	1	4.31	30.88	0.0009	
AC	7.02	1	7.02	50.36	0.0002	
BC	11.29	1	11.29	80.96	<0.0001	
A2	81.21	1	81.21	582.39	<0.0001	
B2	271.96	1	271.96	1950.31	<0.0001	
C2	417.21	1	417.21	2991.99	<0.0001	
Residual	0.98	7	0.14			
Lack of Fit	0.8	3	0.27	5.91	0.0595	
Pure Error	0.18	4	0.045			
Total	896.39	16				

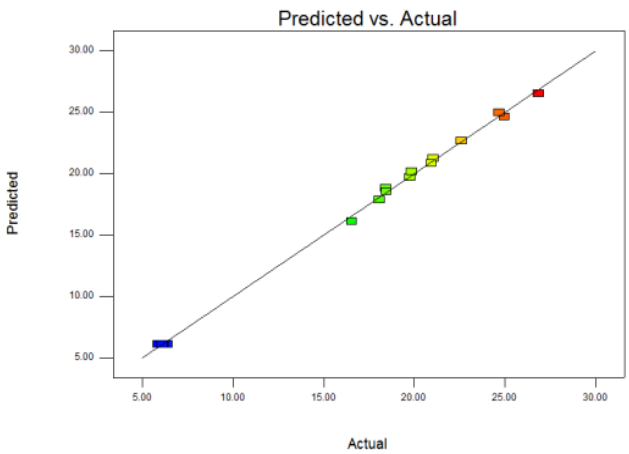

Figure 3. Experimental response values versus predicted response value of Fe^{3+} content.

3.1.4. Response Surface Diagram and Parameter Optimization of Fe^{3+}

The removal of iron from wastewater is mainly achieved through the precipitation formed by Fe^{3+}. When only PAM and PAC were added, the settling time of this process was long. So in this study, the magnetic powder was added simultaneously with PAM and PAC to improve the process effectively. The response surface diagram of Fe^{3+} in reject water is shown in Figure 4.

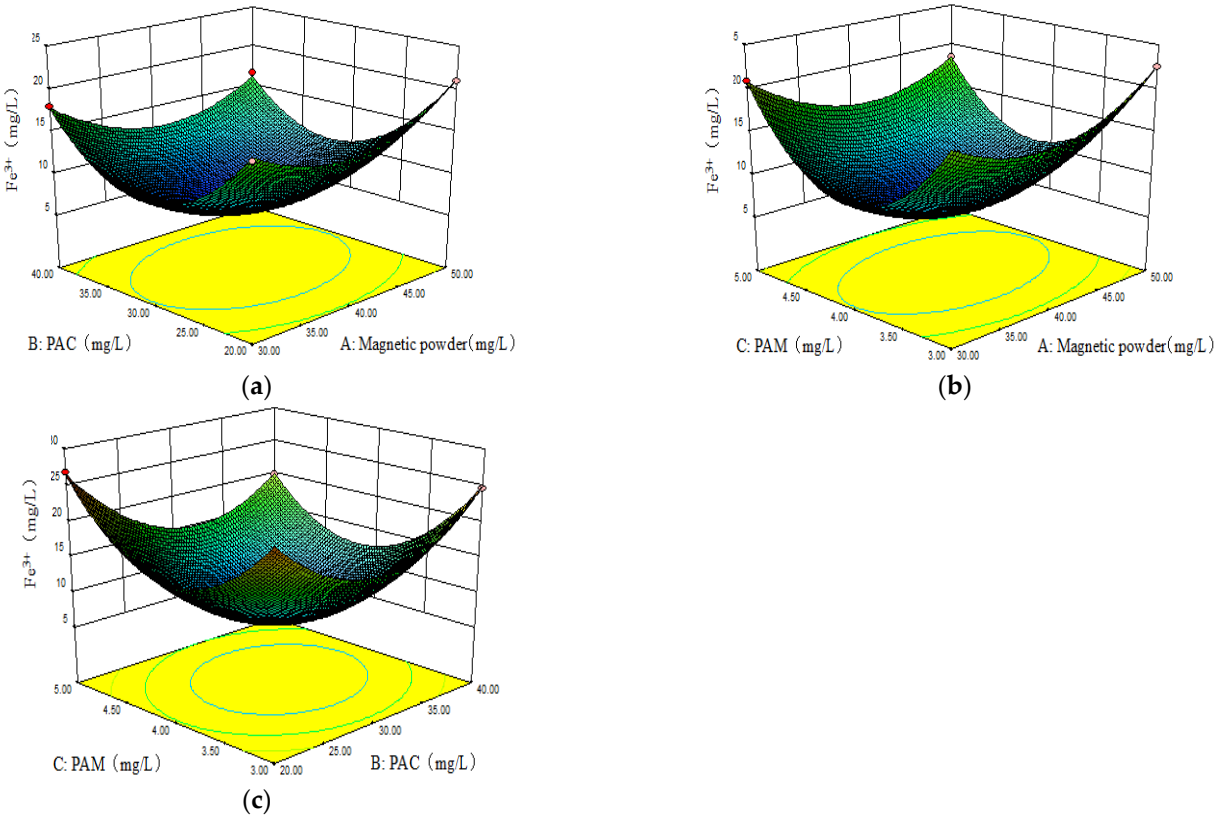

Figure 4. Response surface diagram of interaction among various factors (Fe^{3+}) (**a**) magnetic powder and PAC (**b**) magnetic powder and PAM (**c**) PAC and PAM.

As shown in Figure 4a, when the magnetic powder dosage remained unchanged, at first the Fe^{3+} content in reject water decreased with the increase of PAC, but when PAC continued to increase, the Fe^{3+} content increased instead. When PAC dosage remained unchanged, at first the Fe^{3+} content showed a decreasing trend with the increase in magnetic powder dosage. When PAC exceeds a certain value, Fe^{3+} content increased. The reason coincides with the influence of PAC and magnetic powder dosage on SS removal. As can be seen from Figure 4b, when the PAM dosage remained constant, at first Fe^{3+} content in the sludge dewatering solution decreased with the increase of magnetic powder dosage. However, Fe^{3+} content showed an upward trend when magnetic powder dosage continued to be increased. The reason is that when the magnetic powder dosage was low, the combination of magnetic powder and floc gradually strengthened, and the floc density increased, which improved the floc settling performance and the removal efficiency of Fe^{3+}. When the excessive magnetic powder was added, some magnetic powder was not covered by the floc, and the large floc may have been damaged by shear force because it became a small floc under stirring conditions, which led to a deterioration in the floc's settling performance and reduced the removal efficiency of Fe^{3+} [55,56]. In Figure 4c, when PAC remained unchanged, the Fe^{3+} content first decreased with the increase in PAM dosage. At this time, PAM played a full role of "bridging" on the surface of flocs under the action of internal long chain structure and active groups of PAM, so the Fe^{3+} content in reject water can be effectively removed. The Fe^{3+} content tended to increase after reaching the minimum value, which may be when the PAM concentration was too high, and there was enough PAM on the surface of the floc without other adsorption vacancies. If PAM was added again, the unabsorbed PAM would affect the internal viscosity and repulsion of the reject water, thus affecting the removal efficiency of Fe^{3+} [57–60]. Therefore, the optimal dosage of magnetic powder, PAC and PAM can minimize the content of Fe^{3+} in reject water and achieve the best removal effect.

According to the response surface diagram of Fe^{3+} content in reject water, the influence of the three factors on Fe^{3+} removal is in the order of PAC > PAM > magnetic powder, which is consistent with the result of variance analysis of Fe^{3+} model in Table 5. The order of importance of the three agents is different when treating SS and Fe^{3+}. Because Fe^{3+} has a greater effect on sludge activity, the importance ranking of the three drugs based on Fe^{3+} had a higher priority than that of SS.

3.1.5. Model Validation

In order to achieve the optimal removal effects of SS and Fe^{3+}, the optimal process parameters of the model were obtained through the RSM program: Magnetic powder 40.51 mg/L, PAC 31.31 mg/L and PAM 4.05 mg/L. Under this condition, three validation tests were carried out, and the average value was taken as the final data of the test. The results showed that the SS and Fe^{3+} contents are 9.77 mg /L and 6.21 mg /L respectively, and the removal efficiency is 97.84% and 98.35% respectively. At the same time, the total iron content was 6.98 mg/L. It can meet the requirements of the "Standard for design of outdoor wastewater engineering" (GB50014-2006) that the total influent iron concentration of the biological treatment unit is less than 10 mg/L. The SS and Fe^{3+} contents predicted by the model were 10.03 mg/L and 6.02 mg/L, respectively. The relative error with the model was less than 1%. The results showed that the experimental values were basically consistent with the predicted values, the response surface model was reliable and had practical reference value, and the optimized process parameters can effectively improve the actual removal of SS and Fe^{3+}.

3.2. Particle Size Analysis of Flocs

The floc particle size distribution diagram is a characterization of the change process of floc particle size in the process of flocculation. The trend of the particle size distribution diagram can further explain the change process of floc in the process of magnetic flocculation. The three kinds of flocs treated by (A) PAC, (B) PAC + PAM and (C) magnetic flocculation were respectively taken and injected into the particle size meter by peristaltic pump for particle size analysis, and the particle size diagram in Figure 5 was obtained.

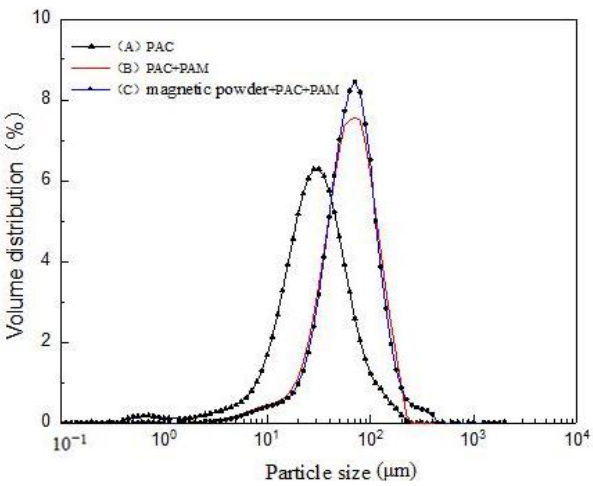

Figure 5. Particle size distribution of flocs.

As can be seen from Figure 5, (B) and (C) had larger particle sizes compared with (A). D_{10}, D_{50} and D_{90} refer to the particle size corresponding to the volume distribution of 10%, 50% and 90%, respectively. The particle size corresponding to D_{50} is usually taken as the average particle size [61,62]. For (A), D_{50} is 28.36 μm, D_{10} is 9.99 μm, and the main mechanism of pollutant removal is electric neutralization. The van der Waals force and electrostatic force are very small, so the strength and particle size of the flocs formed are relatively small [63]. The addition of PAM (as shown in (B)) enhanced the

adsorption bridging effect and promoted the particle size peak to move further to the right. At this time, the peak strength increased significantly. D_{50} was 67.25 μm and D_{10} was 27.67 μm, indicating that the particle size of flocs increased. After adding magnetic powder in conventional coagulation, the floc size distribution was shown in (C). The addition of magnetic powder could promote the particle size peak to move further to the right, and to increase the peak strength, D_{50} was 76.56 μm and D_{10} was 33.30 μm. Compared with (A), the average floc size expanded 3 times, this suggested that as the magnetic powder dosing quantity increased, the floc size increased gradually. Moreover, the particle size distribution was more concentrated. All of these characteristics led to the improvement of the sedimentation performance of flocs [64].

3.3. SEM Analysis of Flocs

The morphology and structure of flocs are the key factors of this study, which can reflect the degree of apparent clarification of effluent water quality and is an important index for evaluating the flocculation phenomenon. In order to further study the reaction mechanism and flocculation effect of magnetic flocculation, the morphology and structure of flocs were observed by scanning electron microscope. The more compact and larger the flocs, the higher the removal rate of pollutants. After adding (a) PAC, (b) PAC + PAM and (c) magnetic powder + PAC + PAM, the morphology and state of flocs were shown in Figure 6.

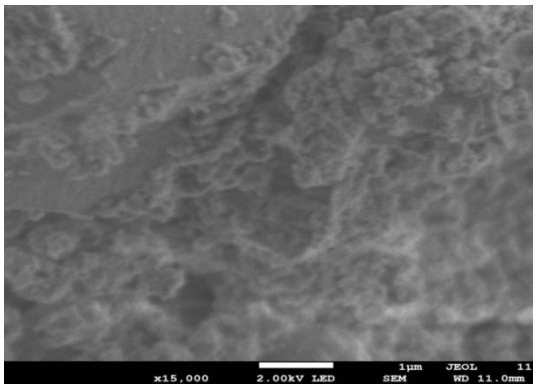

(**a**)

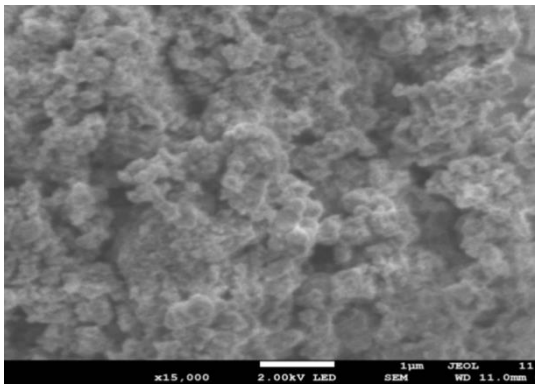

(**b**)

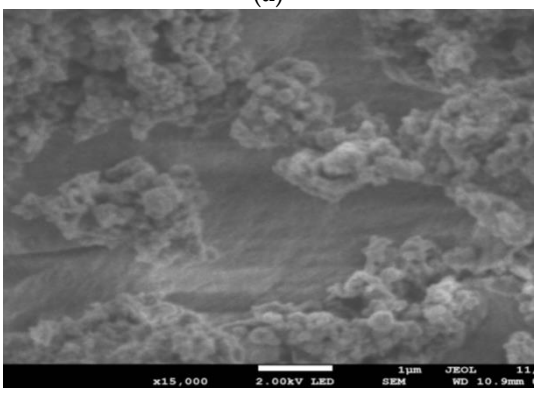

(**c**)

Figure 6. SEM images of flocs (**a**) PAC (**b**) PAC + PAM (**c**) magnetic flocculation.

As shown in Figure 6, the flocs added with PAC were small in volume and dispersed in structure, with smooth surfaces and fluffy and unsubstantial flocs (Figure 6a). As a kind of polymer coagulant, PAM promoted small flocs to form large clusters in series by adsorption bridging (Figure 6b). Compared with the flocs formed by conventional coagulation methods, the flocs treated by magnetic flocculation enhancement technology had a rough surface, larger volume, pores in many places, more obvious adhesion and closer connection (Figure 6c). In the process of coagulation, the magnetic powder would

fully contact with flocs to improve the effective collision between particles. At the same time, the magnetic powder also became the core of coagulation, forming magnetic flocs with Fe_3O_4 as the skeletons. The flocs were intertwined with each other, which increased the size and density of the flocs. So the flocs had stronger impact resistance, and this strengthened the removal effect of pollutants [65,66].

3.4. FTIR Analysis of Flocs

In the reject water treated by magnetic flocculation, the supernatant showed a whitening state. In order to conduct a qualitative analysis of the whitening substances in the supernatant, the drying substances in the supernatant treated by (A) PAC, (B) PAC + PAM and (C) magnetic flocculation were analyzed by Fourier transform infrared spectroscopy, as shown in Figure 7.

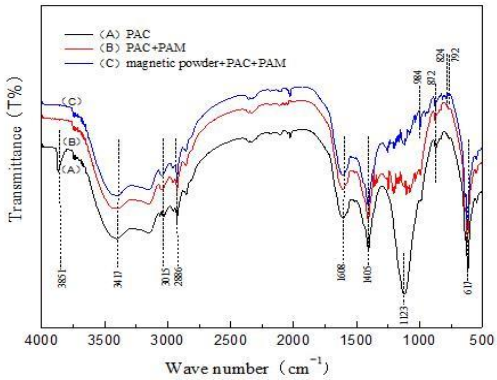

Figure 7. FTIR of flocs treated by three methods.

According to the infrared spectrum in Figure 7, the composition of three kinds of flocs can be obtained. In Figure 7, the absorption peak at 3417 cm^{-1} had a wide peak type, which was the hydroxyl association peak of hydrogen bond formation and had good characteristics of the hydroxyl complex. The peak at 3015 cm^{-1} and 2886 cm^{-1} was caused by C-H stretching, and there was an obvious peak at 1608 cm^{-1}. This was because there were amino compounds in the flocs [67]. The absorption peak at 1405 cm^{-1} was due to the superposition of functional groups of humic acids in the floc [68].

As shown in Figure 7, the three kinds of flocs had an obvious peak of =C-H on the aromatic ring at 872 cm^{-1}, and there was no significant difference in the bending vibration of the peak, while the flocs with magnetic flocculation had an obvious absorption peak at 984 cm^{-1}. This was related to the out-of-plane vibration of =C-H in the olefin, forming the stable monomer structure of Fe-O-Al [69]. In addition, the peak of Al-O in flocs was obvious at 617 cm^{-1}. At the same time, the strong vibration peak of Al-O-Al at 1123 cm^{-1} in PAC was weakened, while the absorption peak of Fe-O-Al and Fe-OH in magnetic flocculation was 824 cm^{-1} and 792 cm^{-1}, respectively. This indicates that the addition of magnetic powder and PAM enhances the hydrolysis process of PAC, increases the charge neutralization and hydrogen bond adsorption process, and forms a more stable flocculation structure, and the volume of the flocs coated with magnetic powder increases significantly. Finally, the flocs sedimentation performance has been effectively improved [70].

3.5. Influence of D_{2f} of Flocs on FA

The fractal theory was first proposed by Professor Mandelbort in the 1970s and introduced into the field of coagulation in the 1980s, which has been widely used in various fields of water treatment [39]. The fractal dimension of flocs can reflect the structural characteristics of flocs to a certain extent. The larger the value of D_{2f} is, the denser the flocs are. Conversely, the smaller the D_{2f} value is, the looser the flocs structure formed [71]. The morphology and surface properties of flocs are the key factors affecting the flocculation pro-

cess, so it is necessary to further study the influence of fractal dimension on the flocculation sedimentation performance in order to obtain better experimental results [47,72].

The specific fitting results of the test are shown in Figure 8. In Figure 8, D_{2f} is the slope of the line.

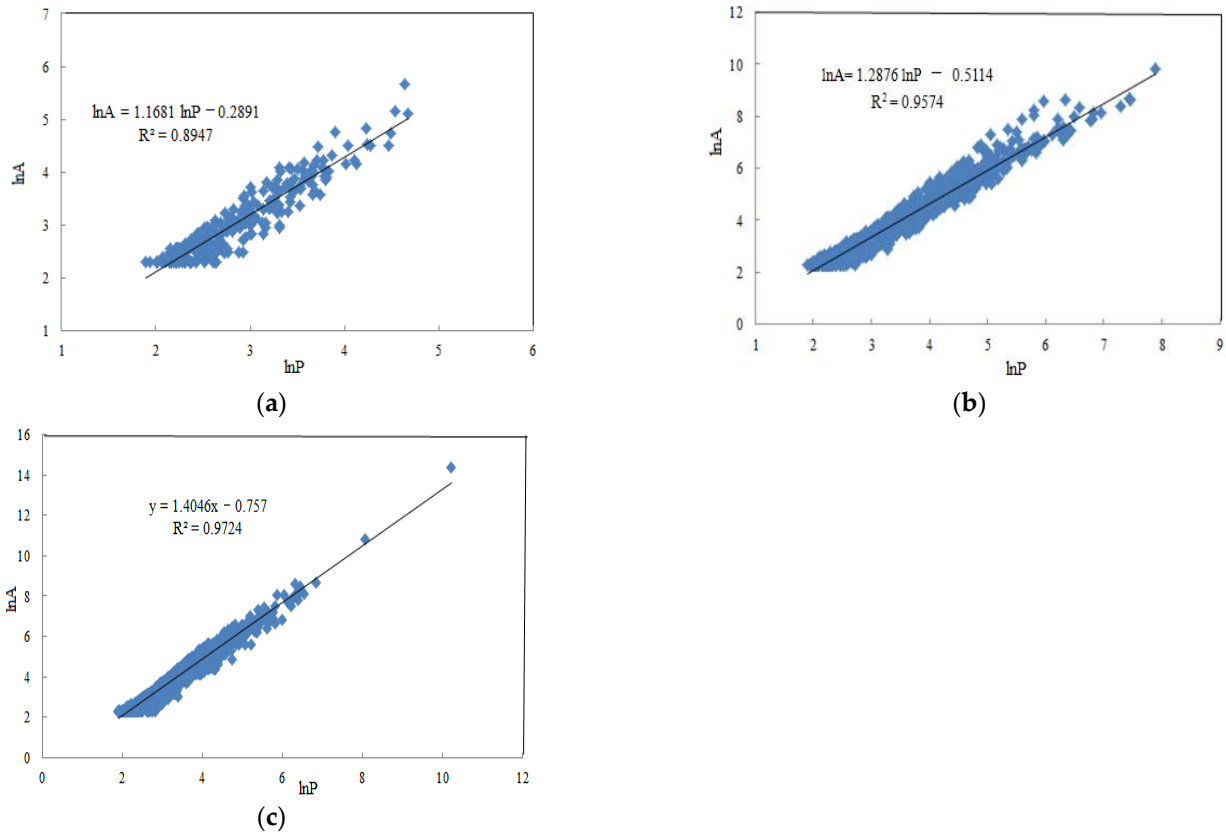

Figure 8. D_{2f} values of flocs treated by three methods (**a**) PAC (**b**) PAC + PAM (**c**) magnetic flocculation.

Figure 8 showed that the D_{2f} of the three flocs treated by (A) PAC, (B) PAC + PAM and (C) magnetic powder + PAC + PAM were 1.1681, 1.2876 and 1.4046 respectively. The linear correlation coefficients of the fitting are 0.8947, 0.9574 and 0.9724 respectively. The linear correlation coefficient of flocs fitting after magnetic flocculation treatment was greater than 0.97, indicating that the magnetic flocs selected in the test had obvious fractal structure [67]. Figure 8a showed that when only PAC was added, the flocs formed irregular shapes and multi-branched loose structures [73,74]. Figure 8b showed that when PAC and PAM were added, the average density of flocs increased and the degree of irregular shape decreased. Compared with Figure 8a, D_{2f} increased significantly. In Figure 8c, when magnetic powder, PAC and PAM were added, the value of D_{2f} of flocs appeared the maximum value, indicating that compared with flocs in Figure 8a,b, flocs at this time were more compact and had the lowest irregular shape. This is consistent with the SEM results of the three kinds of flocs in Section 3.2, further indicating the influence of magnetic particles on the morphology and structure of flocs.

Flocculation is a process in which suspended particles in water gather and gradually form large flocs. After the flocs settle, solid-liquid separation is realized. FA is closely related to the value of the fractal dimension. The surface properties of flocs treated by PAC, PAC + PAM and magnetic flocculation were determined, as shown in Table 6. The D_{2f} and FA of flocs treated by different methods in the table were significantly different.

Table 6. Floc index parameters of three treatment methods.

Methods	D_{2f}	FA
PAC	1.1681 ± 0.0851	0.1762 ± 0.0221
PAC + PAM	1.2876 ± 0.1092	0.2534 ± 0.0523
Magnetic flocculation	1.4046 ± 0.0936	0.4425 ± 0.0345

D_{2f} and FA of the three kinds of flocs were combined to explore the relationship between D_{2f} and FA, as shown in Figure 9. According to Figure 9, the FA of flocs increased with the increase of D_{2f}. Generally speaking, compact flocs had a large D_{2f} value. If the D_{2f} value decreased, the FA value also decreased. According to the test results, when D_{2f} gradually increased from 1.15 to 1.45, FA can increase by 2.6 times. There was a positive correlation between them (R^2 = 0.9839). Through the analysis of D_{2f} and FA, it is further proved that compared with the previous two methods, magnetic flocculation can improve the D_{2f} and FA, and thus improve the floc size and sedimentation performance.

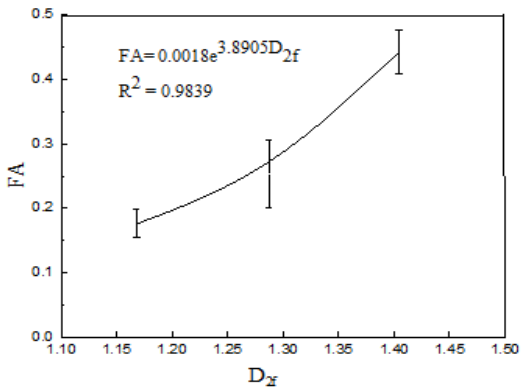

Figure 9. Influence of D_{2f} of flocs on FA.

4. Conclusions

In summary, the simultaneous removal of Fe^{3+} and SS in the anaerobic digestion reject water by the magnetic flocculation technology could be feasible. The RSM was employed to optimize operating conditions for the magnetic flocculation process and to evaluate the effects of three main factors, the dosages of magnetic powder, PAC, and PAM. The optimum conditions for Fe^{3+} and SS removal efficiency were 40.51 mg/L magnetic powder, 31.31 mg/L PAC, and 4.05 mg/L PAM. Under such conditions, the optimal removal efficiencies for Fe^{3+} and SS were 98.35% and 97.84%, respectively. An accurate predicted method of RSM was established to optimize the magnetic flocculation process for the removal of Fe^{3+} and SS from reject water involving the above three influencing parameters. Compared with PAC and PAC + PAM flocs, the magnetic flocculation flocs were large and compact with a larger D_{2f} value, resulting in the disruption of large flocs (average particle size 76.56 μm). As a result, the present study revealed the excellent and efficient removal of Fe^{3+} and SS at the same time by the magnetic flocculation process. The total iron concentration after treatment can meet the requirements of the "Standard for design of outdoor wastewater engineering" (GB50014-2006) that the total influent iron concentration of the biological treatment unit is les. as than 10 mg/L. The RSM was a powerful tool for optimizing operational parameters. The magnetic flocculation process could be a potential method to eliminate Fe^{3+} and SS from the anaerobic digestion reject water.

Author Contributions: Investigation, B.X. and Y.D.; Writing—original draft, B.X.; Data curation, Y.C. (Yongzhi Chi), Y.C (Yiyang Chi), C.F. and B.X.; Methodology, B.X. and Y.C. (Yiyang Chi); Funding acquisition, Y.C. (Yongzhi Chi) and J.Z.; Software, B.X., Y.C. (Yiyang Chi) and J.Z.; Writing—review and editing, J.Z., X.W. and S.T.; Supervision, Y.D. All authors have read and agreed to the published version of the manuscript.

Funding: This research was funded by the Technology Research and Development Program of Tianjin, China (No. 22YFXTHZ00080), the National Key R&D Program of China (No. 2019YFE0122400).

Data Availability Statement: All data are provided as tables and figures.

Acknowledgments: We are thankful to Yuan Li, Hongli Zhang and Liang Zhang for their assistance with analysis of water samples.

Conflicts of Interest: The authors declare no conflict of interest.

References

1. Chynoweth, D.P.; Owens, J.M.; Teixeire, A.A.; Pullammanappallil, P.; Luniya, S.S. Anaerobic digestion of space mission wastes. *Water Sci. Technol.* **2022**, *53*, 177–185. [CrossRef] [PubMed]
2. Pierkiel, A.; Lanting, J. Membrane-coupled anaerobic digestion of municipal sewage sludge. *Water Sci. Technol.* **2005**, *52*, 253–258. [CrossRef] [PubMed]
3. Jung, S.Y.; Kim, M.J.; Lee, J.Y.; Shin, J.H.; Shin, S.G.; Lee, J.Y. Effect of magnetite supplementation on mesophilic anaerobic digestion of phenol and benzoate: Methane production rate and microbial communities. *Bioresour. Technol.* **2022**, *350*, 126943. [CrossRef]
4. Rousseau, P.; Steyer, J.-P.; Volcke, E.I.P.; Bernet, N.; Beline, F. Combined anaerobic digestion and biological nitrogen removal for piggery wastewater treatment: A modelling approach. *Water Sci. Technol.* **2008**, *58*, 133–141. [CrossRef]
5. Li, X.-C.; Peng, Y.-Z.; Zhang, J.-W.; Du, R. Multiple roles of complex organics in polishing THP-AD filtrate with double-line anammox: Inhibitory relief and bacterial selection. *Water Res.* **2022**, *216*, 118373. [CrossRef]
6. Gil, K.I.; Choi, E. Nitrogen removal by recycle water nitritation as an attractive alternative for retrofit technologies in municipal wastewater treatment plants. *Water Sci. Technol.* **2004**, *49*, 39–46. [CrossRef]
7. Ahn, Y.H.; Choi, H.C. Autotrophic nitrogen removal from sludge digester liquids in up flow sludge bed reactor with external aeration. *Process Biochem.* **2006**, *41*, 1945–1950. [CrossRef]
8. Cao, J.; Xie, Y.; Fang, F.; Hu, H. Influences of Fe^{3+} on phosphorus removal andmicrobial products in denitrifying phosphorus removal system. *Res. Environ. Sci.* **2015**, *28*, 125–133.
9. Mena, N.P.; Bulteau, A.L.; Salazar, J.; Hirsch, E.C.; Núñez, M.T. Effect of mitochondrial complex I inhibition on Fe–S cluster protein activity. *Biochem. Biophys. Res. Commun.* **2011**, *409*, 241–246. [CrossRef] [PubMed]
10. Zhang, L.; Zhang, M.; You, S.; Ma, D.; Zhao, J.; Chen, Z. Effect of Fe^{3+} on the sludge properties and microbial community structure in a lab-scale A^2O process. *Sci. Total Environ.* **2021**, *780*, 146505. [CrossRef]
11. Chen, Y.L.; Sui, Q.W.; Yu, D.W.; Zheng, L.B.; Chen, M.X.; Ritigala, T.; Wei, Y.S. Development of a short-cut combined magnetic coagulation-sequence batch membrane bioreactor for swine wastewater treatment. *Membranes* **2021**, *11*, 83. [CrossRef]
12. Lackner, S.; Gilbert, E.M.; Vlaeminck, S.E.; Joss, A.; Horn, H.; van Loosdrecht, M.C.M. Full-scale partial nitritation/anammox experiences: An application survey. *Water Res.* **2014**, *55*, 292–303. [CrossRef] [PubMed]
13. Fan, W.; Liu, X.; Cheng, Y.; Qin, Y.; Yang, S.; Lu, Z.; Liu, Y.; Cao, Q.; Zheng, L. Two-dimensional metal-organic framework nanobelts for selective Fe3+ removal from aqueous solution with high adsorption capacity. *Sep. Purif. Technol.* **2020**, *239*, 116559. [CrossRef]
14. Ozaki, H.; Sharma, K.; Saktaywin, W. Performance of an ultra-low-pressure reverse osmosis membrane (ULPROM) for separating heavy metal: Effects of interference parameters. *Desalination* **2002**, *144*, 287–294. [CrossRef]
15. Nemati, M.; Hosseini, S.M.; Shabanian, M. Novel electrodialysis cation exchange membrane prepared by 2-acrylamido-2-methylpropane sulfonic acid; heavy metal ions removal. *J. Hazard. Mater.* **2017**, *337*, 90–104. [CrossRef] [PubMed]
16. Lv, M.; Zhang, Z.H.; Zeng, J.Y.; Liu, J.F.; Sun, M.C.; Yadav, R.S.; Feng, Y.J. Roles of magnetic particles in magnetic seeding coagulation-flocculation process for surface water treatment. *Sep. Purif. Technol.* **2019**, *212*, 337–343. [CrossRef]
17. Shirakawa, D.; Shirasaki, N.; Matsushita, T.; Matsui, Y.; Yamashita, R.; Matsumura, T.; Koriki, S. Evaluation of reduction efficiencies of pepper mild mottle virus and human enteric viruses in full-scale drinking water treatment plants employing coagulation-sedimentation–rapid sand filtration or coagulation–microfiltration. *Water Res.* **2022**, *213*, 118160. [CrossRef]
18. Kapoor, J.K.; Jabin, S.; Bhatia, H.S. Optimization of coagulation-flocculation process for food industry waste water treatment using polyelectrolytes with inorganic coagulants. *J. Indian Chem. Soc.* **2015**, *92*, 1697–1703.
19. Bosak, V.K.; Vanderzaag, A.C.; Crolla, A.; Kinsley, C.; Chabot, D.; Miller, S.S.; Gordon, R.J. Treatment of potato farm wastewater with sand filtration. *Environ. Technol.* **2016**, *37*, 1597–1604. [CrossRef]
20. Lee, W.C.; Chang, C.C. Effectively recycling swine wastewater by coagulation-flocculation of nonionic polyacrylamide. *Sustainability* **2022**, *14*, 1742. [CrossRef]
21. Lipus, L.C.; Krope, J.; Crepinsek, L. Dispersion destabilization in magnetic water treatment. *J. Colloid Interface Sci.* **2001**, *236*, 60–66. [CrossRef] [PubMed]
22. Lisa, T.; Jason, L.S.; Andrew, H. Depositional remanent magnetization: Toward an improved theoretical and experimental foundation. *Earth Planet. Sci. Lett.* **2006**, *244*, 515–529.

23. Noor, M.H.M.; Wong, S.; Ngadi, N.; Inuwa, I.M.; Opotu, L.A. Assessing the effectiveness of magnetic nanoparticles coagulation/flocculation in water treatment: A systematic literature review. *Int. J. Environ. Sci. Technol.* **2021**, *19*, 6935–6956. [CrossRef]
24. Wang, C.; Wang, Y.-J.; Ouyang, Z.-Z.; Shen, T.T.; Wang, X.K. Preparation and characterization of polymer-coated Fe_3O_4 magnetic flocculant. *Sep. Sci. Technol.* **2018**, *53*, 814–822. [CrossRef]
25. Chen, X.-Y.; Zheng, H.-L.; Xiang, W.-Y.; An, Y.Y.; Xu, B.C.; Zhao, C.L.; Zhang, S.X. Magnetic flocculation of anion dyes by a novel composite coagulant. *Desalination Water Treat.* **2019**, *143*, 282–294. [CrossRef]
26. Bai, S.J.; Li, C.-L.; Fu, X.-Y.; Wu, M.; Wen, S.-M. Beneficiation of micro-fine magnetic minerals from reductive iron ore with ultrafine grinding-magnetic flocculation separation. *Sep. Sci. Technol.* **2018**, *53*, 136–145. [CrossRef]
27. Luo, L.-Q.; Nguyen, A.V. A review of principles and applications of magnetic flocculation to separate ultrafine magnetic particles. *Sep. Purif. Technol.* **2017**, *172*, 85–99. [CrossRef]
28. Han, S.-F.; Jin, W.-B.; Tu, R.-J.; Gao, S.-H.; Zhou, X. Microalgae harvesting by magnetic flocculation for biodiesel production: Current status and potential. *World J. Microbiol. Biotechnol.* **2020**, *36*, 7. [CrossRef]
29. Chen, Y.Q.; Luo, M.; Cai, W.-F. Influence of operating parameters on the performance of magnetic seeding flocculation. *Environ. Sci. Pollut. Res.* **2016**, *23*, 2873–2881. [CrossRef]
30. Dai, K.; Chen, P.; Wang, Z.C. Magnetic composite $Ca(OH)_2/Fe_3O_4$ for highly efficient flocculation in papermaking black liquor without pH neutralization. *Adv. Powder Technol.* **2021**, *32*, 2457–2468. [CrossRef]
31. Zhang, Z.; Yang, Y.L. Experimental study on deep treatment of coking wastewater by magnetic flocculation. *Ind. Water Wastewater* **2012**, *43*, 25–29.
32. Zielinski, M.; Rusanowska, P.; Debowski, M.; Hajduk, A. Influence of static magnetic field on sludge properties. *Sci. Total Environ.* **2018**, *625*, 738–742. [CrossRef] [PubMed]
33. Xu, B.; Chi, Y.-Z.; Zhang, H.-L.; Zhao, J.-H.; Ding, Y.-M.; Zhang, Y.-F.; Li, Y.-Y. Enhanced treatment of anaerobic digestion reject water by magnetic flocculation technology. *Chem. Ind. Eng. Prog.* **2020**, *39*, 4693–4701.
34. Bajpai, M.; Katoch, S.S. Techno-economical optimization using Box-Behnken (BB) design for chemical oxygen demand and chloride reduction from hospital wastewater by electro-coagulation. *Water Environ. Res.* **2020**, *92*, 2140–2154. [CrossRef]
35. Yu, Y.-Y.; Sun, J.; Zhou, J.; Chen, A.; Shah, K.J. Preparation and characterization of high-efficiency magnetic heavy metal capture flocculants. *Water* **2021**, *13*, 1732. [CrossRef]
36. Andrews, S.; Nover, D.; Schladow, S.G. Using laser diffraction data to obtain accurate particle size distributions: The role of particle composition. *Limnol. Oceanogr. Methods* **2010**, *8*, 507–526. [CrossRef]
37. Liu, M.; Qin, X.-L.; Yuan, J.-L.; Qiu, Y.; Tang, S.-H. Preparation, Characterization and decolorization performance of magnetic adsorbent pellets formed by the utilization of electric flocculation sludge. *Chemistryselect* **2021**, *6*, 7285–7294. [CrossRef]
38. Chin, C.J.; Lu, S.C.; Yiacoum, S.; Tsouris, C. Fractal dimension of particle aggregates in magnetic fields. *Sep. Sci. Technol.* **2004**, *39*, 2839–2862. [CrossRef]
39. Mandelbrot, B.B. *The Fractal Geometry of Nature*; Freeman and Company: New York, NY, USA, 1982; pp. 1–60.
40. Meakin, P. *Fractal Scaling and Growth Far from Equilibrium*; Cambridge University Press: London, UK, 1998; p. 83.
41. Jin, B.; Wilén, B.M.; Lant, P. A comprehensive imsight into floc characteristics and their impact on compressibility and settleability of activated sludge. *Chem. Eng. J.* **2003**, *95*, 221–234. [CrossRef]
42. Yu, W.-Z.; Gregory, J.; Yang, Y.-L.; Sun, M.; Liu, T.; Li, G.-B. The effect of coagulation and applied breakage shear on the re-growth of kaolin flocs. *Environ. Eng. Sci.* **2010**, *27*, 483–492. [CrossRef]
43. Chakraborti, R.K.; Gardner, K.H.; Atkinson, J.F.; Van Benschoten, J.E. Changes in fractal dimension during aggregation. *Water Res.* **2003**, *37*, 873–883. [CrossRef] [PubMed]
44. Jorand, F.; Zartarian, F.; Thomas, F.; Block, J.C.; Manem, J. Chemical and structural (2D) linkage between bacteria within a within activated sludge flocs. *Water Res.* **1995**, *29*, 1639–1647. [CrossRef]
45. Mietta, F.; Chassagne, C.; Verney, R.; Winterwerp, J.C. On the behavior of mud floc size distribution: Model calibration and model behavior. *Ocean Dyn.* **2011**, *61*, 257–271. [CrossRef]
46. Wu, M.-Y.; Yu, W.-Z.; Qu, J.-H.; Gregory, J. The variation of flocs activity during floc breakage and aging, adsorbing phosphate, humic acid and clay particles. *Water Res.* **2019**, *155*, 131–141. [CrossRef]
47. Wilén, B.M.; Jin, B.; Lant, P. The influence of key chemical constituents in activated sludge on surface and flocculating properties. *Water Res.* **2003**, *37*, 2127–2139. [CrossRef]
48. Peng, S.-L.; Jiang, G.-C.; Li, X.-L.; Yang, L.-L.; Liu, F.; He, Y.-B. Flocculation of submicron particles in water-based drilling fluids by CMC-g-DMDAAC. *J. Pet. Sci. Eng.* **2018**, *162*, 55–62. [CrossRef]
49. Chin, C.J.; Chen, P.-W.; Wang, L.-J. Removal of nanoparticles from CMP wastewater by magnetic seeding aggregation. *Chemosphere* **2006**, *63*, 1809–1813. [CrossRef]
50. Liu, Z.-M.; Li, X.; Zhan, P.; Hu, F.-P.; Ye, X. Removal of cadmium and copper from water by a magnetic adsorbent of PFM: Adsorption performance and micro-structural morphology. *Sep. Purif. Technol.* **2018**, *206*, 199–207. [CrossRef]
51. Liu, Z.-M.; Zhang, Z.; Hu, F.-P.; Duan, X.-Y.; Ye, X. Adsorption performance and micro-structural morphology of a novel magnetic composite adsorbent for removing Cd^{2+} from water. *Microchem. J.* **2019**, *146*, 1209–1217. [CrossRef]
52. Mao, Y.-H.; Chang, Q.; Zeng, L.-Y. Velocity field structure and flocculation efficiency in Taylor-Couette flow. *Sep. Sci. Technol.* **2013**, *48*, 659–663. [CrossRef]

53. Wang, Y.; Zhang, F.; Chu, Y.-B.; Gao, B.-Y.; Yue, Q.-Y. The dye or humic acid water treatment and membrane fouling by polyaluminum chloride composited with sodium alginate in coagulation-ultrafiltration process. *Water Sci. Technol.* **2013**, *67*, 2202–2209. [CrossRef]
54. Zhang, H.; Li, Y.-L.; Wu, X.-G.; Zhang, Y.-J.; Zhang, D.-B. Application of response surface methodology to the treatment landfill leachate in a three-dimensional electrochemical reactor. *Waste Manag.* **2010**, *30*, 2096–2102. [CrossRef] [PubMed]
55. Kang, S.; Li, Q.; Wu, Z.; Zhang, H.; Zheng, L.; Wei, Y. Study on characteristics and mechanism of magnetic coagulationfor pollutants removal in black and odorous water. *Technol. Water Treat.* **2021**, *47*, 24–28.
56. Zhang, C.; Xu, D.; Kang, S.; Li, C.; Zheng, L.; Wei, Y. The application and coagulation mechanism of magnetic coagulation in treating mixed sewage from small towns. *Acta Sci. Circumstantiae* **2022**, *42*, 268–278.
57. Ma, J.-Y.; Xia, W.; Fu, X.; Ding, L.; Kong, Y.-L.; Zhang, H.-W.; Fu, K. Magnetic flocculation of algae-laden raw water and removal of extracellular organic matter by using composite flocculant of Fe_3O_4/cationic polyacrylamide. *J. Clean. Prod.* **2020**, *248*, 119276. [CrossRef]
58. Zhao, Y.; Liang, W.-Y.; Liu, L.-J.; Li, F.-Z.; Fan, Q.-L.; Sun, X.-L. Harvesting *Chlorella vulgaris* by magnetic flocculation using Fe_3O_4 coating with polyaluminium chloride and polyacrylamide. *Bioresour. Technol.* **2015**, *198*, 789–796. [CrossRef]
59. Song, W.-Z.; Zhang, Y.; Yu, J.-W.; Gao, Y.-X.; Naitoc, T.; Oinumac, G.; Inanagac, Y.; Yang, M. Rapid removal of polyacrylamide from wastewater by plasma in the gas-liquid interface. *J. Environ. Sci.* **2019**, *83*, 1–7. [CrossRef]
60. Ye, S.-X.; Feng, P.; Zhang, W. Rapid solidification of Portland cement/polyacrylamide hydrogel (PC/PAM) composites for diverse wastewater treatments. *Rsc Adv.* **2020**, *10*, 18936–18944. [CrossRef]
61. Guérin, L.; Coufort-Saudejaud, C.; Liné, A.; Frances, C. Dynamics of aggregate size and shape properties under sequenced flocculation in a turbulent Taylor-Couette reactor. *J. Colloid Interface Sci.* **2017**, *491*, 167–178. [CrossRef]
62. Bai, S.-J.; Wen, S.-M.; Liu, D.-W.; Zhang, W.-B. Separation of phosphorus and magnetic mineral fines from siderite reductive ore by applying magnetic flocculation. *Sep. Sci. Technol.* **2014**, *49*, 1434–1441. [CrossRef]
63. Zhang, Y.-L.; Liu, P.-K.; Xiao, L.-J.; Zhang, Y.-K.; Yang, X.-H.; Jiang, L.-Y. Experimental study on flocculation effect of tangential velocity in a cone-plate clarifier. *Separations* **2021**, *8*, 105. [CrossRef]
64. Zhou, L.-B.; Han, Y.-X.; Li, W.-B.; Zhu, Y.-M. Study on polymer-bridging flocculation performance of ultrafine specular hematite ore and its high gradient magnetic separation behavior: Description of floc microstructure and flocculation mechanism. *Sep. Purif. Technol.* **2021**, *276*, 119304. [CrossRef]
65. Edzwald, J.K.; Tobiason, J.E. Enhanced coagulation: US requirements and a broader view. *Water Sci. Technol.* **1999**, *40*, 63–70. [CrossRef]
66. Fu, J.-H.; Han, H.-S.; Wei, Z.; Sun, W.; Yue, T. Recovery of ultrafine scheelite particles by magnetic seeding flocculation and its mechanism. *Colloids Serfaces A Hysicochemical Eng. Asp.* **2021**, *628*, 127266. [CrossRef]
67. Wang, J.; Yang, J.; Zhang, H.-W.; Guo, W.-S.; Ngo, H.H. Feasibility study on magnetic enhanced flocculation for mitigating membrane fouling. *J. Ind. Eng. Chem.* **2015**, *26*, 37–45. [CrossRef]
68. Zularisam, A.W.; Ismail, A.F.; Salim, M.R.; Sakinah, M.; Hiroaki, O. Fabrication, fouling and foulant analyses of asymmetric polysulfone (PSF) ultrafiltration membrane fouled with natural organic matter (NOM) source waters. *J. Membr. Sci.* **2007**, *299*, 97–113. [CrossRef]
69. Ma, M.; Zhang, Y.; Yu, W.; Shen, H.-Y.; Zhang, H.-Q.; Gu, N. Preparation and characterization of magnetite nanoparticles coated by amino silane. *Colloids Surf. A: Physicochem. Eng. Asp.* **2003**, *212*, 219–226. [CrossRef]
70. Tang, J.; Wang, J.; Jia, H.; Wen, H.-T.; Li, J.; Liu, W.-B.; Li, J.-Y. The investigation on Fe_3O_4 magnetic flocculation for high efficiency treatment of oily micro-polluted water. *J. Environ. Manag.* **2019**, *24*, 399–407. [CrossRef]
71. Zhao, Y.Q. Correlations between floc physical properties and optimum polymer dosage in alum sludge condtioning and dewatering. *Chem. Eng. J.* **2003**, *92*, 227–235. [CrossRef]
72. Liao, B.-Q.; Allen, D.G.; Droppo, I.G. Surface properties of sludge and their role in bioflocculation and settleability. *Water Res.* **2001**, *35*, 339–350. [CrossRef]
73. Karatasou, S.; Santamouris, M. Detection of low-dimensional chaos in buildings energy consumption time series. *Commun. Nonlinear Sci. Numer. Simul.* **2010**, *15*, 1603–1612. [CrossRef]
74. Liu, F. Study on focculation kinetics based on coagulation and precipitation integration process. Master's Thesis, Harbin Institute of Technology, Harbin, China, 2011.